J Appl Electrochem (2012) 42:689–698
DOI 10.1007/s10800-012-0412-6

ORIGINAL PAPER

Locomotion determined and controlled by electrochemical networks

A robotic application based on electrochemical oscillations

Antonis Karantonis · Stavroula Koutalidi

Received: 8 February 2012 / Accepted: 4 April 2012 / Published online: 28 April 2012

Abstract In the present work the modes of four-legged locomotion generated and controlled by a network of coupled electrochemical oscillatory electrode pairs are explored. Each pair, operating under constant potential conditions, consists of an iron disk (anode) and a copper coil (cathode) and all pairs are immersed in a common electrolytic bath (1 M H_2SO_4 and 0.4 M $CuSO_4$). The electrochemistry of the system is studied and the conditions of oscillatory and synchronous firing are determined. The current response of each pair is determined by the geometry of the network: if the interactions are between the iron anodes then the oscillations are synchronized in-phase whereas if the interactions are between iron anodes and copper cathodes the oscillations are out-of-phase. The electric pulses produced by the network are supplied to a prototype, specially designed mechanical system where possible modes of four-legged locomotion are observed.

Keywords Electrochemical oscillations · Electrochemical network · Synchronization · Locomotion

1 Introduction

The movement of many biological systems is based on the rhythmic movement of their limbs, which are controlled by the nervous system. The existence of neural rhythms is an unambiguous phenomenon but their exact role and functioning in the living organisms is still an open problem. The frequency and phase-difference of neural signals which carry information to specific organs may be the most important features determining the response of these organs [1, 2]. Moreover, the locomotion of living organisms is often determined by a a central pattern generator (CPG), that is, a neural network able to produce rhythmic outputs even in the absence of feedback [3–6].

The neural signals are electric pulses created by the passage of ionic currents through the neural membrane and traveling along the neural axis. Neural cells become members of the neural system, or specific neural centers, through the synapses which allow the communication between neurons [7]. The functioning of the neural cell can be described, in some degree, by purely electrochemical processes which occur during the generation and propagation of neural signals [8]. Therefore, it is assumed that, in principle, electrochemical systems must exist which are capable of mimicking the neural response [9].

Indeed, a variety of electrochemical systems are capable of producing high amplitude electric pulses, either autonomously or under perturbation, and behave as oscillators or excitators. Moreover, these systems have the ability to communicate through the electrolytic solution while in proximity and thus form networks [10–12] capable of various types of synchronization [13]. Moreover, electrochemical oscillatory networks have been considered as information processing units and pattern recognition devices [14, 15].

The aim of the present work is to investigate the ability of electrochemical oscillatory networks to function as CPGs. The novelty of this work is based on the fact that a real physicochemical experimental system (acting as a

Electronic supplementary material The online version of this article (doi:10.1007/s10800-012-0412-6) contains supplementary material, which is available to authorized users.

A. Karantonis (✉) · S. Koutalidi
Department of Materials Science and Engineering, School of Chemical Engineering, National Technical University of Athens, 15780 Zografou, Athens, Greece
e-mail: antkar@central.ntua.gr

neural control system) is combined with a mechanical device able to manifest locomotion. This way the modes of four-legged locomotion are explored while generated and controlled by a network of coupled electrochemical oscillatory electrodes, Fe | 1 M H_2SO_4, 0.4 M $CuSO_4$| Cu, i.e. pairs of iron disk (anode) and a copper coil (cathode) immersed in a common electrolytic bath (1 M H_2SO_4 and 0.4 M $CuSO_4$). This versatile system offers the ability to easily form networks of different geometries due to the absence of a third (reference) electrode [10]. At the first stage, the electrochemistry of the system is studied by potentiodynamic, potentiostatic and electrochemical impedance spectroscopy measurements and the conditions of sustained current oscillations are determined. Then, the current response of the network is explored under different geometries in order to realize in-phase and out-of-phase synchronous firing of the network elements. The electric pulses produced by the network are supplied to a mechanical system consisting of four electric motors connected to four independent wheels. The back-forth and left-right movement is independent due to a specially designed chassis. The modes of locomotion of this mechanical system are explored in relation to the phase difference between the autonomous electrochemical pulses.

2 Experimental

Anodic polarization measurements, potentiostatic and open circuit experiments were performed in a three electrode arrangement using an EG&G 263 A potentiostat. An iron disk of 1 mm diameter (Sigma-Aldrich 99.9+ %) was used as a working electrode whereas a copper coil made from approx. 20 cm of 1 mm diameter copper wire (Aldrich 99.9+ %) was used as a counter electrode. A SCE was utilized as reference electrode. To solution was made from H_2SO_4 (Fisher Scientific, analytical reagent grade) and $CuSO_4$ (Panreac, PA). Impedance spectroscopy measurements were performed by a Solartron 1260 impedance / phase gain analyzer.

Coupling experiments were performed under a two electrode arrangement where an iron disk of 1 mm diameter was used as an anode and a copper coil (approx. 20 cm copper wire) was used as a cathode. The potential difference between the electrode pairs was controlled by a galvanically isolated multi-channel potential source. The geometry of the network of electrodes i.e. the relative position of the electrodes, was fixed by using a specially designed matrix.

The current response of the electrode pairs was recorded and simultaneously supplied to the motors of a home-made robotic device via an amplifier. The robotic device, Fig. 1, consisted of a chassis carrying four electric motors. Two motors were located at the front and two at the back of the chassis. The front and back part of the chassis were connected by a spring and two articulated axes in order to achieve independence along the x (back-forth) and y (right-left) direction. Each motor was connected to a wheel whose rotation was determined by the signal arriving from the electrochemical network.

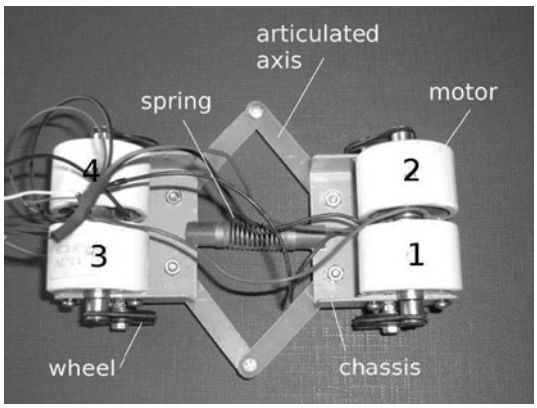

Fig. 1 The robotic device

3 Results and discussion

3.1 Electrochemistry of the system

The aim of this section is to present the qualitative features of the electrochemical processes, mainly in relation to the system dynamics. Detailed electrochemical studies of systems where similar phenomena are observed can be find elsewhere [16–18]. When an iron electrode is immersed in sulfuric acid solution, the electrode potential is determined by the process of iron dissolution and proton reduction, occurring simultaneously on the electrode surface. In a solution containing also copper cations, the electrode potential is shifted to more anodic values and the corrosion current increases due to the relative values of the standard redox potentials of copper and hydrogen. As a result, an additional process occurs, namely, the deposition of copper on iron surface.

The dissolution of iron and deposition of copper will proceed until the electrode surface is almost completely covered by copper and the open circuit potential is shifted to that of a copper electrode immersed in a solution of copper ions. The evolution of these phenomena can be seen in Fig. 2. After immersion of the Fe electrode in the 1 M H_2SO_4, 0.4 M $CuSO_4$ solution, the open circuit potential is −0.420 V, a value more anodic than that observed in the absence of copper ions. At this stage (stage A) iron dissolution and copper deposition take place occur. As copper deposition proceeds the electrode surface is covered by

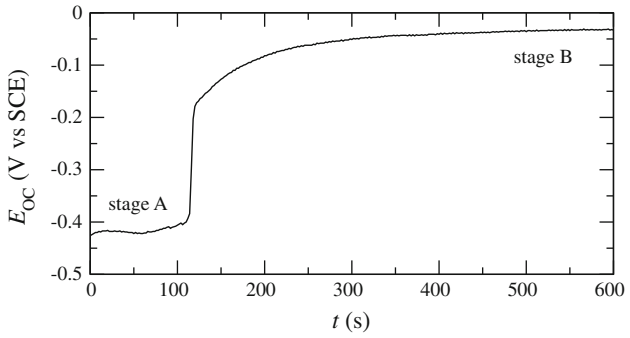

Fig. 2 Time evolution of the open circuit potential for a Fe electrode in 1 M H_2SO_4, 0.4 M $CuSO_4$

copper and the electrode potential approaches −0.04 V, a value close to the one expected by the Nernst equation for the $Cu^{2+} + 2e \rightleftharpoons Cu$ redox couple (stage B).

The occurrence of these reactions and the formation of a copper layer on the iron surface modify the shape of the current-potential curve recorded when the iron electrode is polarized anodically. Moreover, the shape of the polarization curve depends on the extend of copper deposition on the electrode surface. In Fig. 3a the forward scan of the anodic polarization curve of the Fe | 1 M H_2SO_4 system is presented for comparison reasons. Thus, in the absence of copper ions in the solution, active electrodissolution is observed in the region from open circuit potential −0.490 to −0.210 V, ferrous salt precipitation for −0.210 to 0.230 V and oxide passivation for potentials more anodic than 0.230 V [19, 20]. The forward scan of the anodic polarization curve of the Cu | 1 M H_2SO_4, 0.4 M $CuSO_4$ is presented in Fig. 3b, also for comparison reasons. In the region from open circuit potential 0.03 to 0.320 V active dissolution is observed followed by cupric salt precipitation for potentials more anodic than 0.320 V [21].

The case of the Fe | 1 M H_2SO_4, 0.4 M $CuSO_4$ is presented in Fig. 3c just after the immersion of the iron electrode in the electrolytic solution (stage A). As can be seen, the open circuit potential is shifted to the more anodic value of −0.390 V, due to the presence of Cu^{2+} ions acting as oxidizing agents (see Fig. 3a). In spite of the spontaneous deposition of Cu^{2+} ions on the iron electrode surface (observed by visual inspection of the surface) the open circuit potential is shifted anodically but does not correspond to the open circuit potential of a copper electrode immersed in a solution containing copper ions, that is, the electrode is still in stage A of the E_{OC} versus t curve of Fig. 2. This is an indication that copper is deposited on the iron electrode but the deposit is not covering completely the electrode surface. This is evident also by observing the current while the potential is scanned anodically. Thus, from open circuit potential to −0.320 V, active iron dissolution is observed but the total current is substantially

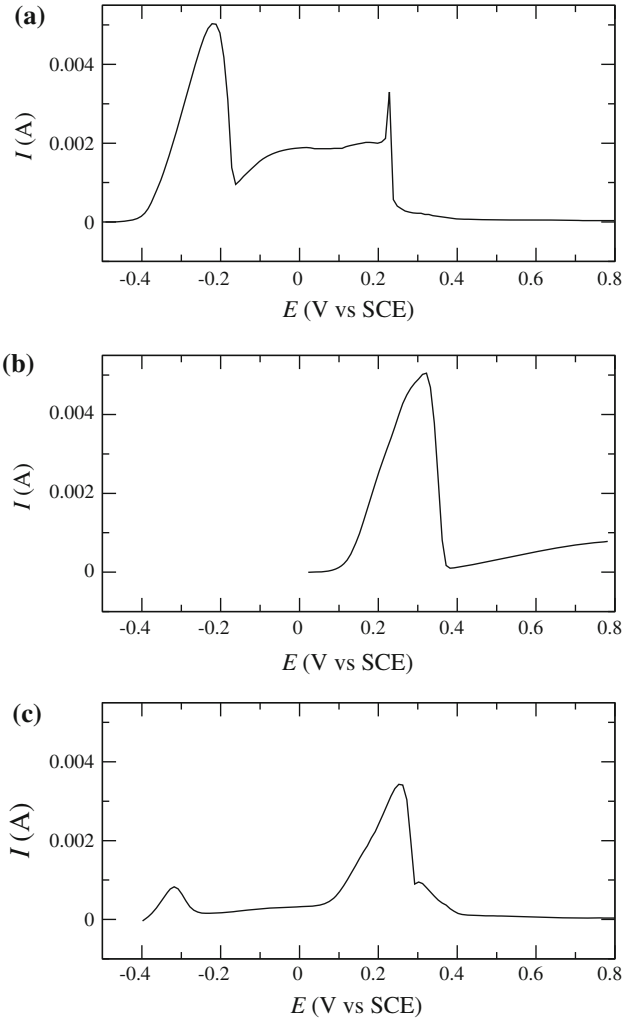

Fig. 3 **a** Anodic polarization of Fe in 1 M H_2SO_4, **b** anodic polarization of Cu in 1 M H_2SO_4, 0.4 M $CuSO_4$, **c** anodic polarization of Fe in 1 M H_2SO_4, 0.4 M $CuSO_4$ just after immersion of the electrode. Scan rate 20 mVs^{-1}

smaller in comparison to that of Fig. 3a due to the simultaneous cathodic current of copper deposition. For potentials more anodic than −0.320 V, ferrous salt precipitation is observed. At 0.07 V the current increases due to the electrodissolution of copper which has been deposited spontaneously on the iron surface. The dissolution continues until all copper is removed at 0.260 V. Further increase of the potential causes the passivation of the free iron surface by an oxide layer.

A curve for the cyclic polarization of the Fe | 1 M H_2SO_4, 0.4 M $CuSO_4$ system just after immersion (stage A) is presented in Fig. 4a. The forward scan is identical with the one described in Fig. 3c whereas during the backward scan the oxide layer is dissolved at 0.260 V and a large current overshoot is observed, corresponding to stable autonomous current oscillations under potentiostatic conditions. Further decrease of the potential results in a

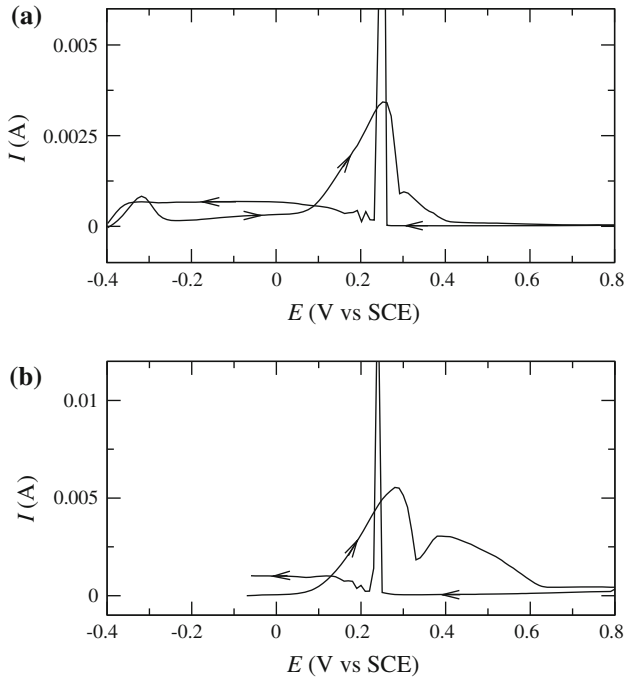

Fig. 4 **a** Anodic polarization of Fe in 1 M H_2SO_4, 0.4 M $CuSO_4$ just after immersion of the electrode, **b** anodic polarization of Fe in 1 M H_2SO_4, 0.4 M $CuSO_4$. Scan rate 20 mVs^{-1}

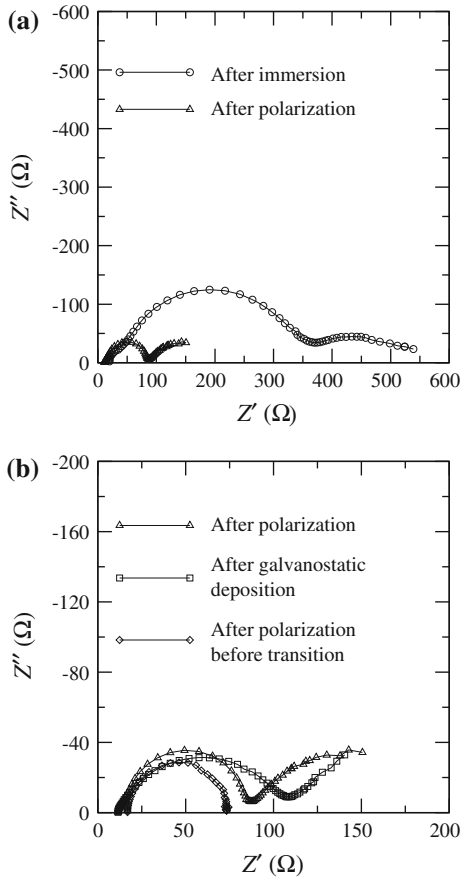

Fig. 5 Impedance of Fe in 1 M H_2SO_4, 0.4 M $CuSO_4$ for **a** a polished electrode at $E_{OC} = -0.035$ V (*circles*) and of a pretreated electrode at $E_{OC} = -0.041$ V (*triangles*) **b** a pretreated electrode at $E_{OC} = -0.041$ V (*triangles*), a polished electrode at $E_{OC} = 0.025$ V after galvanostatic deposition of copper (*squares*) and a pretreated electrode at $E_{OC} = -0.358$ V (*diamonds*)

limiting current due to ferrous salt formation and a final decrease when the open circuit potential is reached. In Fig. 4b the cyclic polarization curve is presented for the same system, but after the electrode reaches an open circuit potential corresponding to a completely deposited copper layer (stage B). Apparently, during the forward scan the copper layer is dissolved whereas during the backward scan a current overshoot is observed once again. Further decrease of the potential is not followed by a decrease of the current at the open circuit potential due to the absence of copper deposits on the iron electrode surface. The above results suggest that the instability observed in the Fe | 1 M H_2 SO_4, leading to periodic oscillations, can occur in the present system when the spontaneously formed copper deposit is removed from the iron electrode surface.

The effect of electrode pretreatment on the surface deposits and reaction rates can be studied by measuring the impedance of the system under open circuit conditions. In Fig. 5a, cycle symbols, the Nyquist plot of the impedance is plotted for a freshly polished iron electrode immersed in 1 M H_2SO_4, 0.4 M $CuSO_4$ solution at stage B, *i.e.* after the open circuit potential have reached a value corresponding to a copper deposited layer, $E_{OC} = -0.035$ V. On the other hand, the Nyquist plot of the impedance on iron electrode in 1 M H_2SO_4, 0.4 M $CuSO_4$ solution after a cyclic scan in the region from open circuit conditions to 0.8 V and a transition to stage B, $E_{OC} = -0.041$ V, is represented by triangle symbols. As can be seen by comparing these two curves, the faradaic resistances of the pretreated system are smaller that those of the freshly polished electrode, indicating that the rates of dissolution and deposition processes are enhanced at the pretreated surface.

The effect of the electrode surface state on the rates of the processes can be seen in the Nyquist plots of Fig. 5b. The impedance of the pretreated electrode at open circuit conditions at stage B ($E_{OC} = -0.041$ V) is represented by triangles. The Nyquist plot corresponds to a corroding iron electrode where a copper deposit is formed. A qualitatively similar Nyquist plot is obtained for an iron electrode where copper is galvanostatically deposited on the surface prior to the impedance measurement (squares) and the open circuit potential corresponds to that of stage B ($E_{OC} = 0.025$ V). Finally, the Nyquist plot of an iron electrode while on stage A ($E_{OC} = -0.358$ V) is represented by diamond symbols. In this case, the plot consists of a single capacitance loop indicating that the amount of copper deposit is small.

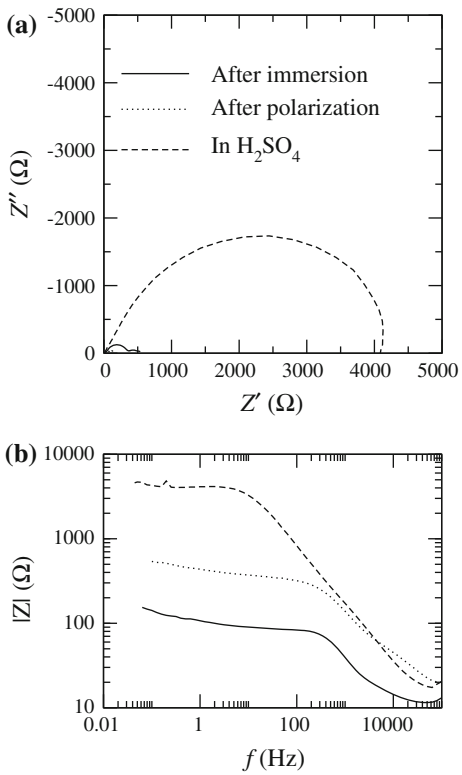

Fig. 6 **a** Nyquist plots and **b** modulus of the impedance of polished Fe in 1 M H_2SO_4, 0.4 M $CuSO_4$ (*solid line*) $E_{OC} = -0.035$ V, of pretreated Fe in 1 M H_2SO_4, 0.4 M $CuSO_4$ (*dotted line*) and pretreated Fe in 1 M H_2SO_4 (*dashed line*)

The effect of the presence of copper ions in the solution can be seen in Fig. 6. The Nyquist plot of a freshly polished iron electrode immersed in H_2SO_4 system (in the absence of copper ions) is shown by the dashed line in Fig. 6a, where $E_{OC} = -0.445$ V. The Nyquist plot of a freshly polished iron electrode at stage B in the presence of copper ions is represented by a dotted line, where $E_{OC} = -0.035$ V. By comparing these two plots it is evident that iron dissolution is enhanced due to the presence of copper ions, as expected. In this figure the Nyquist plot of a pretreated iron electrode at stage B ($E_{OC} = -0.041$ V) is also presented, by the resistance values are very small and the curve is slightly visible. Nevertheless, the changes of polarization resistances can be seen in the plot of the impedance modulus vs. frequency, Fig. 6b. It is evident from this figure that the presence of copper ions as well as pretreatment enhances the dissolution rate of iron.

In order to conclude the electrochemical investigation of the system, a two electrode arrangement was tested in order to verify if a copper coil can act as both counter and reference electrode. Under this arrangement, both auxiliary and reference connections of the potentiostat are shortcut to the copper coil electrode. A typical polarization curve of the Fe | 1 M H_2SO_4, 0.4 M $CuSO_4$| Cu system under these conditions is presented in Fig. 7a. As can be seen, all qualitative features observed under the typical three electrode arrangement are observed also in a two electrode arrangement, but shifted approximately 80 mV cathodically (the value of the $Cu^{2+} + 2e \rightleftharpoons Cu$ redox couple as

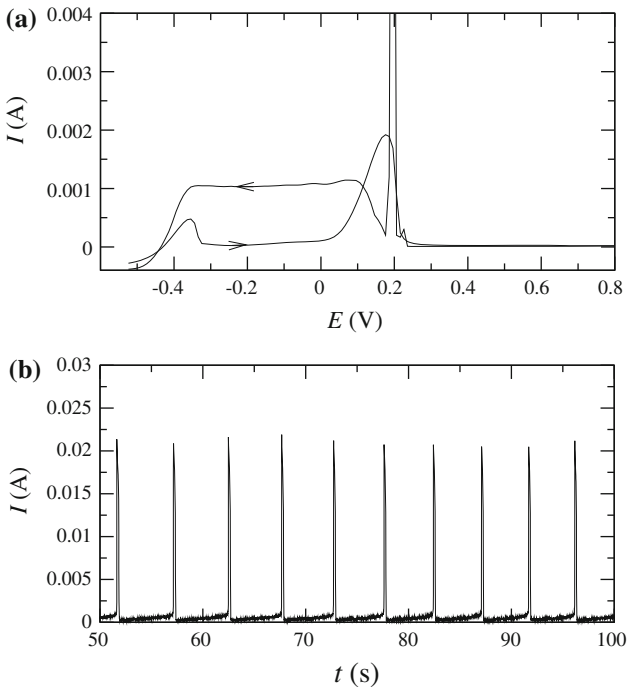

Fig. 7 **a** Polarization curve and **b** potentiostatic measurement at $E = 220$ mV of the Fe | 1 M H_2SO_4, 0.4 M $CuSO_4$| Cu system in a two electrode arrangement

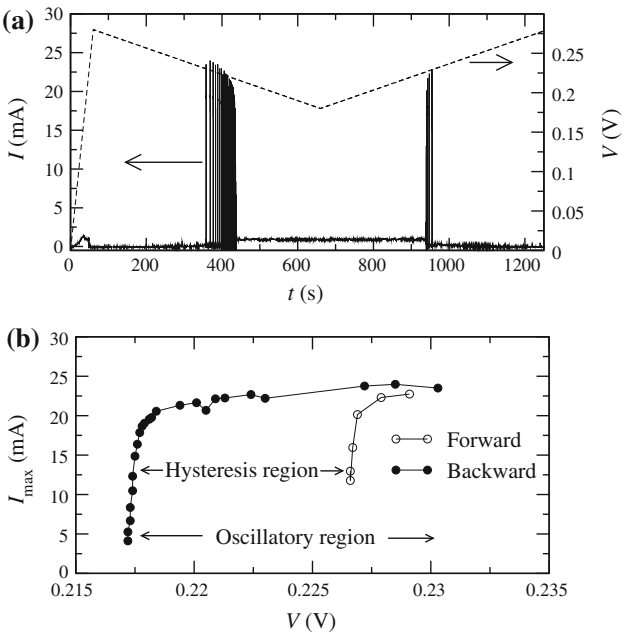

Fig. 8 **a** Current response of the Fe | 1 M H_2SO_4, 0.4 M $CuSO_4$| Cu system under slow scan of the potential difference V for $d = 2.5$ cm and **b** variation of the amplitude of the oscillations

determined by the Nernst equation). A typical potentiostatic measurement under the two electrode arrangement is presented in Fig. 7b for $E = 220$ mV. As can be seen, the current oscillates autonomously with a fixed period, similarly to the case observed in the Fe | 1 M H_2SO_4 system in a three electrode arrangement. The autonomous current oscillations are of relaxation type. During the active stage of the oscillation the current is increased and the electrode surface is almost free. During the silent stage the current is almost zero because of the oxide formation on the electrode surface.

3.2 System dynamics

As shown in Sect. 3.1 the Fe | 1 M H_2SO_4, 0.4 M $CuSO_4$ system exhibits periodic oscillations of the current in a three electrode arrangement. Moreover the current of the Fe | 1 M H_2SO_4, 0.4 M $CuSO_4$| Cu system also oscillates periodically if a copper coil is used as a cathode. Thus, a multi-channel potential source can be used to control the potential difference V between an iron–copper pair. The characteristics of the oscillatory regime of a single iron–copper pair where V between the electrodes is controlled can be revealed by applying a slow cyclic scan of V by a potential source. This procedure is presented in Fig. 8a for an electrode pair where the distance between the electrodes is $d = 2.5$ cm. Initially a rapid scan is applied up to 0.280 V. At this value of V all copper is removed from the iron electrode and the surface is passivated (see Fig. 7a). Then the potential scan is reversed and varied slowly to the value 0.180 V. While V is decreased the current remains at a low value corresponding to the passive state and suddenly starts to oscillate when $V \approx 0.230$ V. Further decrease of V results in a decrease of the oscillations amplitude until $V \approx 0.217$ V where oscillations stop and the state corresponding to the ferrous salt precipitation is recorded (see Fig. 7a). When $V = 0.180$ V the scan is reversed once again and oscillations are recorder when $V \approx 0.226$ V. The amplitude of the oscillations is increasing slightly as V is increased and suddenly oscillations seize at $V \approx 0.230$ V. Apparently, under this arrangement, stable oscillations exist in the region from 0.217 to 0.230 V but a hysteresis region also exists from 0.217 to 0.226 V.

The existence of the oscillatory and hysteresis regions can be visualized by plotting the amplitude of the oscillations I_{max} as a function of the potential difference V. As seen in Fig. 8b, during the forward scan (white circles) oscillations emerge at 0.226 V and seize at 0.230 V. The

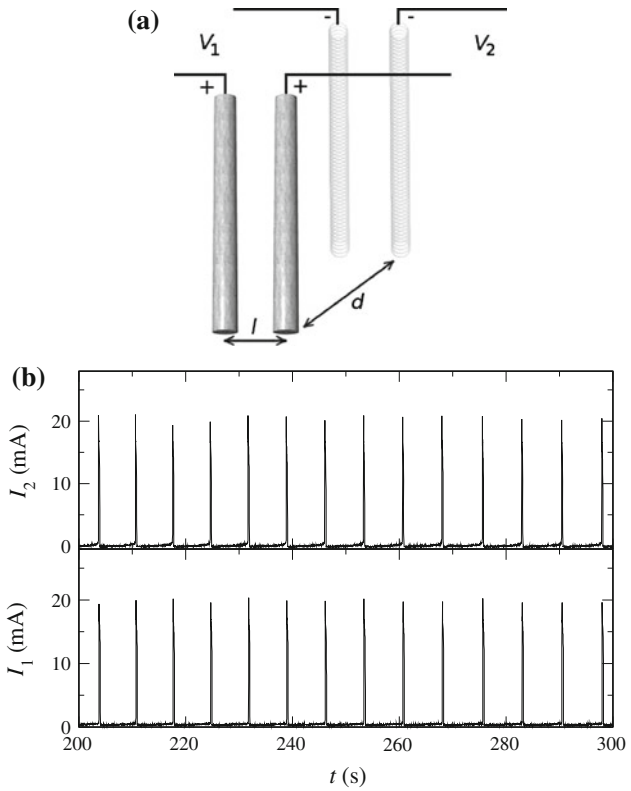

Fig. 9 **a** Schematic representation of a network consisting of two electrode pairs where the interaction is between iron–iron and copper–copper electrodes, and **b** representative in-phase synchronization for $V_1 = V_2 = 225$ mV, $d = 2.5$ cm, $l = 0.5$ cm

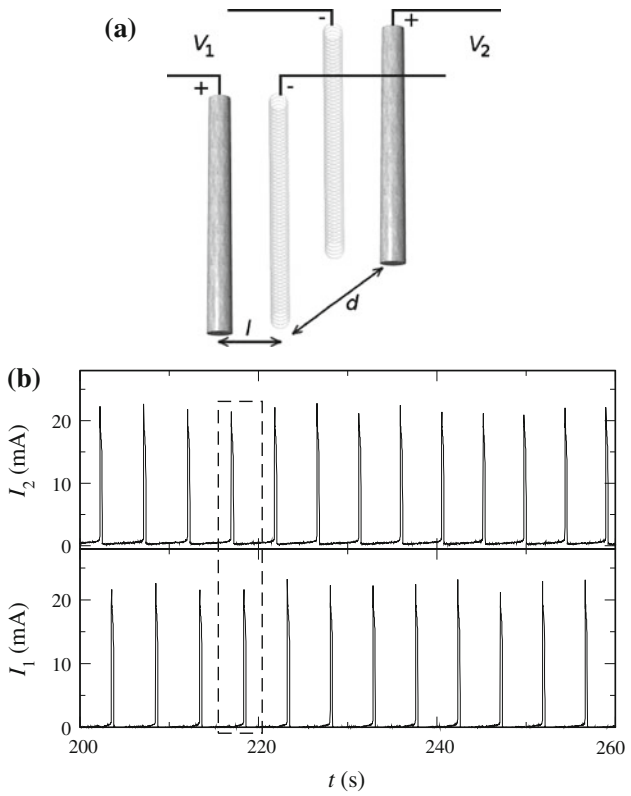

Fig. 10 **a** Schematic representation of a network consisting of two electrode pairs where the interaction is between iron–copper electrodes, and **b** representative out-of-phase synchronization for $V_1 = V_2 = 222$ mV, $d = 2.5$ cm, $l = 0.5$ cm

maximum amplitude observed is about 22 mA. During the backward scan (black circles) oscillations emerge at 0.230 V with amplitude 23 mA and disappear at 0.217 V.

3.3 Synchrony and locomotion

A network of oscillators can be formed by immersing a number of electrode pairs in a common 1 M H_2SO_4, 0.4 M $CuSO_4$ solution and applying a potential difference V_i, within the oscillatory region, to each pair. Due to the relative changes of the potential drops at each interface and the ionic currents in the common solution, oscillatory electrode pairs interact and behave as coupled periodic oscillators. Thus, the network's response depends on the distance l between the interacting electrodes and the geometry of the network, i.e. the relative position of the electrodes.

In Fig. 9a the geometry of a simple network consisting of two oscillatory electrode pairs is shown schematically. The gray rods represent embedded iron wires where only the bottom disk shape part is free to react and springs represent copper coils. In this figure d is the distance between iron and copper electrodes of a pair operating under potential V_i and l is the distance between interacting electrodes. In this specific example, where l is considered smaller than d, interactions are expected between electrodes of the same type, that is, between iron-iron and copper-copper electrodes. Under this configuration each electrode pair exhibits periodic oscillations and due to coupling the period of the oscillations is the same and the phase difference is almost zero, i.e. the oscillators are *synchronized in-phase*. A typical example for $V_1 = V_2 = 225$ mV is presented in Fig. 9b.

The effect of the geometry of the network can be seen in Fig. 10. In this case, the network consists of two electrode pairs but the interaction is between iron and copper electrodes, Fig. 10a. As shown in Fig. 10b for $V_1 = V_2 = 222$ mV, the oscillations are periodic with the same period but a fixed phase difference, *i.e* the oscillators are *synchronized out-of-phase*.

The above modes of synchronization can be observed in networks consisting of more than two electrode pairs. A representative example is shown schematically in Fig. 11a where four electrode pairs are immersed in the electrolytic solution. Under this configuration iron–iron and copper–copper electrodes interact. As a result all oscillators exhibit periodic oscillations with a common period and almost zero phase difference. The network's response for $V_1 = V_2 = V_3 = V_4 = 240$ mV is presented

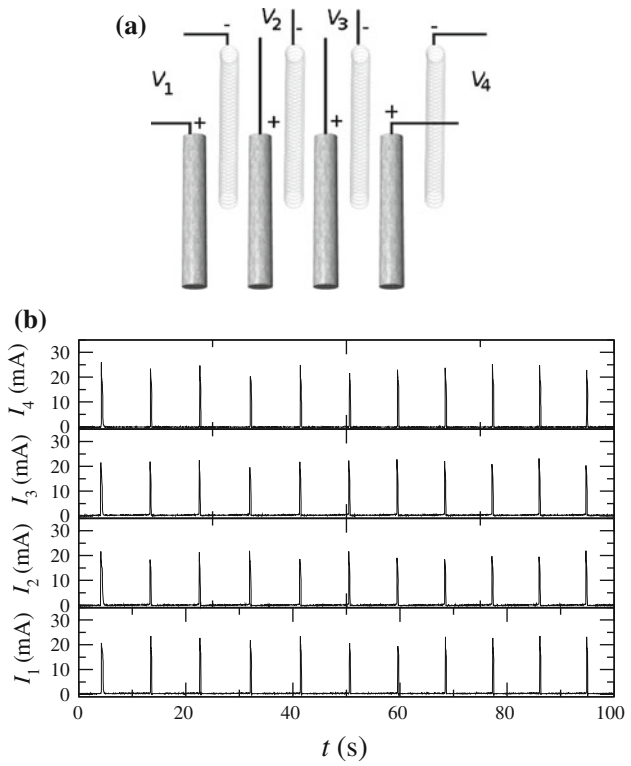

Fig. 11 **a** Schematic representation of a network consisting of four electrode pairs where the interaction is between iron–iron and copper–copper electrodes, and **b** representative in-phase synchronization for $V_1 = V_2 = V_3 = V_4 = 240$ mV, $d = 2.5$ cm, $l = 0.5$ cm

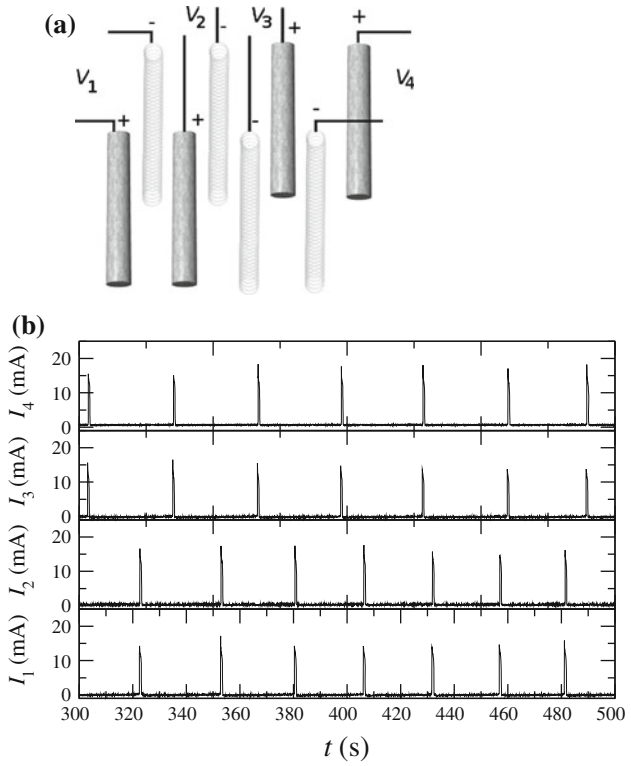

Fig. 12 **a** Schematic representation of a network consisting of four electrode pairs where the interaction is between iron–copper electrodes, and **b** representative synchronization into groups for $V_1 = V_2 = V_3 = V_4 = 240$ mV, $d = 2.5$ cm, $l = 0.5$ cm

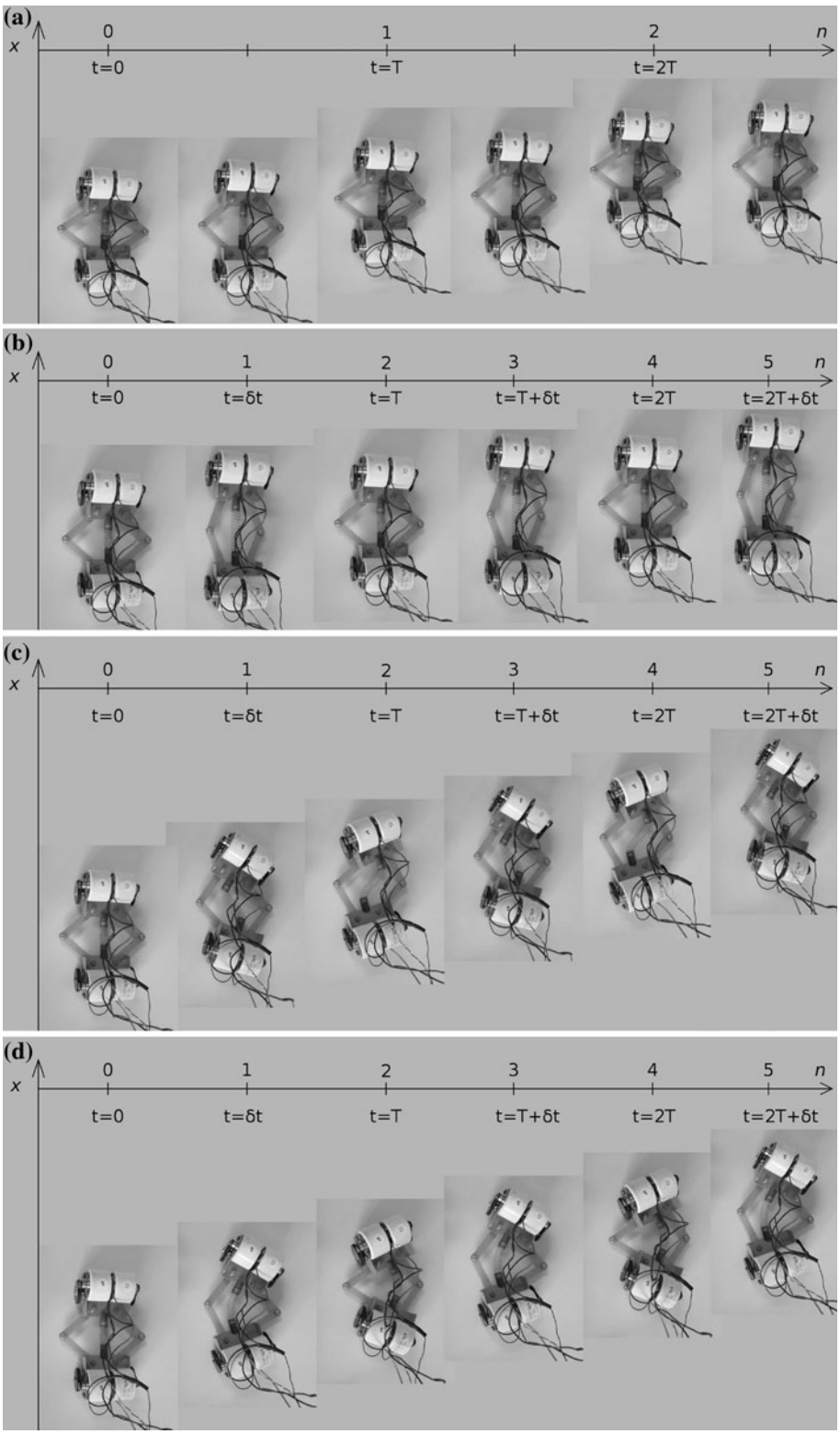

Fig. 13 Modes of locomotion for a robotic device controlled by an electrochemical network of four oscillators. **a** Galloping, **b** jumping, **c** trotting A and **d** trotting B

in Fig. 11b where it is evident that oscillations are synchronized in-phase.

A more peculiar response is observed when the geometry of the network is the one presented in Fig. 12a. Under this configuration the synchronization between pair 1 and 2 is expected to be in-phase. In-phase synchronization is expected for pairs 3 and 4. Nevertheless, due to the interaction between pair 2 and 3, out-of-phase synchronization is to be observed. A representative example for this configuration for $V_1 = V_2 = V_3 = V_4 = 240$ mV is presented

in Fig. 12b. It can be seen that oscillators are separated into groups. Within each group oscillators are synchronized in-phase whereas groups are synchronized out-of-phase.

The ability of a network to form groups of oscillators synchronized out-of-phase can be utilized to control the modes of locomotion of the simple robotic device described in Sect. 2. Hence, for a fixed network geometry, a constant potential V_i is applied to each electrode pair within the oscillatory region. As a result, the oscillations will synchronize according to the geometry of the network. The output of every electrode pair is fed to the input of each motor via the amplifier. Thus, the wheel associated to each motor will rotate only when an oscillatory pulse occurs and remain silent when the oscillator is on the silent stage.

Four different modes of locomotion are expected (see also Electronic Supplementary Information). The first mode, called galloping, corresponds to the case where all oscillators are synchronized in-phase. In this case, all four wheels are expected to rotate almost simultaneously causing the forward movement of the robotic device. Locomotion is achieved in a single stage, within a period T, Fig. 13a

The second mode, called jumping, correspond to the case where pair 1 and 2 are synchronized in-phase, pair 3 and 4 are synchronized in-phase but groups are synchronized out-of-phase. In this case two wheels are expected to rotate simultaneously (e.g the two wheels at the front of the device) while the other two wheels (e.g. the two wheels at the back of the device) remain silent. After a time interval δt, corresponding to the phase difference between groups, the other two wheels will rotate while the former are silent. As a result, locomotion is achieved in two stages within a period T, Fig. 13b

The third more, called trotting A, correspond to the case where pair 1 and 4 are synchronized in-phase, pair 2 and 3 are synchronized in-phase but groups are synchronized out-of-phase. In this case two wheels are expected to rotate simultaneously (e.g the left front and the left back wheels of the device) while the other two wheels (e.g. the right front and the right back wheel of the device) remain silent. After a time interval δt, corresponding to the phase difference between groups, the other two wheels will rotate while the former are silent. As a result, locomotion is achieved in two stages within a period T, Fig. 13c

The final mode, called trotting B, correspond to the case where pair 1 and 3 are synchronized in-phase, pair 2 and 4 are synchronized in-phase but groups are synchronized out-of-phase. In this case two wheels are expected to rotate simultaneously (e.g the left front and the right back wheels of the device) while the other two wheels (e.g. the right front and the left back wheel of the device) remain silent. After a time interval δt, corresponding to the phase difference between groups, the other two wheels will rotate while the former are silent. As a result, locomotion is achieved in two stages within a period T, Fig. 13d

4 Conclusions

Two processes take place on the anode surface during the anodic polarization of the Fe | 1 M H_2SO_4, 0.4 M $CuSO_4$| Cu system, namely the dissolution/passivation of iron and the dissolution/deposition of copper. The dynamics depend on the presence of copper deposits on the iron electrode. When a copper layer is formed, autonomous current oscillations are suppressed whereas when the copper layer is dissolved the current exhibits oscillations of relaxation type within a defined potential window. A network of electrochemical oscillators, consisting of pairs of iron/copper electrodes, is synchronized either in-phase or out-of-phase. The type of synchronization is determined by the geometry of the network, i.e. the relative position of anode and cathodes. Moreover, due to synchronization, grouping is observed, that is, separation of oscillators into groups where the group members are synchronized in-phase whereas groups are synchronized out-of-phase. The synchronization and grouping ability of the network makes it capable of acting as a CPG. This CPG is determining and controlling the modes of locomotion of a simple robotic system. The different modes of locomotion are (a) galloping, (b) trotting type A, (c) trotting type B and (d) jumping. It is concluded that simple electrochemical networks can produce specific oscillatory patterns, determined by the network's geometry, corresponding to different modes of locomotion of simple mechanical systems.

References

1. Ijspeert A (2000) Virtual worlds vol 1834, Lecture notes in computer science. Springer, Berlin, pp 225–234
2. Ijspeert A, Crespi A, Cabelguen JM (2005) Neuroinformatics 3:171
3. Cohen A (1987) J Neurosci Meth 21:113
4. Kopell N, Ermentrout G (1988) Math Biosci 90:87
5. Sigvardt K, Williams T (1992) Semin Neurosci 4:37
6. Taga G (1998) Biol Cybern 78:9
7. Hoppensteadt F, Izhikevich E (1997) Weakly connected neural networks vol 126, Applied mathematical sciences. Springer-Verlag, New York
8. Dayan P, Abbott L (2001) Theoretical neuroscience: computational and mathematical modeling of neural systems. The MIT Press, Cambridge
9. Amatore C, Brown A, Thouin L, Warkocz JS (1998) CR Acad Sci Paris IIC 1:509
10. Karantonis A, Miyakita Y, Nakabayashi S (2002) Phys Rev E 65:046213
11. Miyakita Y, Karantonis A, Nakabayashi S (2002) Chem Phys Lett 362:461

12. Karantonis A, Koutsaftis D, Kouloumbi N (2009) Electrochim Acta 55:374
13. Karantonis A, Pagitsas M, Miyakita Y, Nakabayashi S (2004) J Phys Chem B 108:5836
14. Sadeghi S, Thompson M (2010) Phys Chem Chem Phys 12:6795
15. Sadeghi S, Thompson M (2010) BioSystems 102:99
16. Agrawal R, Kapool M (1982) J S Afr Inst Min Metall 82:106
17. Wei W, Lee C, Chen H (1994) Langmuir 10:1980
18. Alemany C, Diard JP, Gorrec BL, Montella C (1996) Electrochim Acta 41:1483
19. Pagitsas M, Sazou D, Karantonis A, Georgolios C (1992) J Electroanal Chem 327:93
20. Sazou D, Karantonis A, Pagitsas M (1993) Int J Bifurc Chaos 3:981
21. Alkire R, Cangellari A (1989) J Electrochem Soc 136:913